

## Extract of *Angelica sinensis* as oilfield corrosion inhibitor for mild steel in H<sub>2</sub>SO<sub>4</sub> media

Ambrish Singh\*, Yin Caihong, Yang Yaocheng

School of Materials Science and Engineering, Southwest Petroleum University, Xindu district, Chengdu city-610500, Sichuan province, China.

\*E-mail: [vishisingh4uall@gmail.com](mailto:vishisingh4uall@gmail.com); [drambrishsingh@gmail.com](mailto:drambrishsingh@gmail.com)

Received: 7 July 2019 / Accepted: 3 September 2019 / Published: 29 October 2019

---

The root extract of *Angelica sinensis* (AS) was examined as potential corrosion inhibitor of mild steel in 1 M sulphuric acid (H<sub>2</sub>SO<sub>4</sub>) media using weight loss, electrochemical and surface studies. *Angelica sinensis* has its medicinal importance in Chinese traditional medicine since ancient time. It is used to cure several diseases and most important one includes the anemia in women. So, this medicinal herb is chosen as naturally friendly corrosion inhibitor for mild steel in sulphuric acid, as it is easily available, cheap and easy to use. The weight loss results discovered that samples covered with AS showed less weight loss compared to the samples without AS. The electrochemical tests including electrochemical impedance spectroscopy (EIS), and potentiodynamic polarization (PDP) showed good mitigation efficiency of AS in 1 M H<sub>2</sub>SO<sub>4</sub> media. The mixed shift of the anodic and cathodic slopes advised that the AS represented as mixed category. The surface studies were completed using scanning electron microscopy (SEM) and contact angle. Both the studies displayed even surface in existence of AS and rough surface in its absence. The kinetic and thermodynamic parameters were also calculated. All the experimental results are in decent pact respectively.

---

**Keywords:** *Angelica sinensis*, H<sub>2</sub>SO<sub>4</sub>, Mild steel, Corrosion inhibition, EIS, SEM

### 1. INTRODUCTION

Mild steel is preferred all over the world owing its small price and availability. It could be used as a suitable material for oil field storage tanks, transportation pipelines, boilers etc. [1]. The storage tanks store oil for a long period of time. To enhance oil recovery, the tanks are washed with acidizing solutions. Sometimes, to remove the clots or precipitations on the internal side of transportation pipelines they are treated with acidic solutions. These acidizing solutions may cause severe corrosion in the storage tanks, pipelines or oilfield reservoir [2]. This could further lead to accidents, failures and complete shutdown of the place. Internal corrosion is very difficult to measure or to keep a regular watch as the

blisters can develop beneath the coating of the pipeline and can grow severely with time. The depth of the pitting or uniform corrosion will increase extensively if not treated well in time. The corrosion will start to form more pits and cracks throughout the area leading to the failures and accidents. So, there is always a need to develop compounds that can be mixed with acidizing solution to mitigate corrosion during the acidization process.

Although, many corrosion mitigating technique exists, but use of inhibitors is widely used and best practice to effectively mitigate corrosion process. It is of both pragmatic and theoretical importance. Inhibitors are used in pickling, descaling and cleaning processes to reduce the corrosion rate of the metals. Now, due to strict regulation from the governments and environment regulatory boards the existing compounds cannot be used in higher concentration due to their toxicity level. Adding these substances in lower concentration may not work always depending on the size of the tanks. It is cheap, easily applicable and requires simple instruments. So in order to develop and test ecofriendly compounds, extraction of substances from plants being natural, without toxicity was conducted. Several authors have conducted similar tests and have obtained good results as oilfield inhibitor [3-10]. The achieved results exhibited that plant extracts could function as potential corrosion inhibitors.

Plant extracts are significant as they are ecologically benign and renewable foundation for an extensive variety of desirable mitigators. Natural extracts are regarded as an extremely ironic source of biological mixtures that can be separated by modest techniques with small price. Although, well recognized that inhibition takes place through adsorption of AS particles on the steel surface. The adsorption can further reflect the nature of inhibition efficiency of the inhibitor depending on chemical, mechanical, physical, and structural properties under given circumstances [11].

*A. sinensis* is a herb from the family of Apiaceae that grows in cool elevated peaks in China, Japan, and Korea. It is also known as dong quai Chinese: 当归) or "female ginseng" with its peculiar yellowish brown root. It is believed to be used for more than thousand years in traditional medicine and is beneficial for women's health. The medicine prepared from the roots of *A. sinensis* provides several remedies to diseases such as anemia, osteoarthritis, infections, high blood pressure, cardiovascular conditions, headache, fatigue, and inflammation. *A. sinensis* is rich in various naturally occurring chemical compounds including flavonoids, polysaccharides, sterols, ferulate, ligustilide, p-cymene, butylphthalide, cnidilide, and isoenidilide. Due to these chemicals in the extract better mitigating effect is seen for the corrosion of mild steel in acidic media. Since, we are focusing on the extract so no methods were employed to separate the components or to study them separately. Natural images of *A. sinensis* are shown in Fig. 1. The present work explores the impeding outcome of root extracts of female ginseng (*Angelica sinensis*) (AS) on the mild steel corrosion in 1 M H<sub>2</sub>SO<sub>4</sub> media using the weight loss, electrochemical and surface methods.



**Figure 1.** Natural image of *A. sinensis* (picture from book chapter by: Liu Dongling et. al [12])

## 2. EXPERIMENTAL SECTION

Mild steel samples of specified dimensions were used for all the tests. The mild steel samples were prepared as test electrodes embedded in epoxy resin with open  $1 \text{ cm}^2$  area for electrochemical experiments. The visible surface was rubbed with SiC abrasive paper (different grades), washed carefully and dried prior to use. The acidic solution of  $1 \text{ M H}_2\text{SO}_4$  was organized from analytical rated  $\text{H}_2\text{SO}_4$  and distilled water. AS was prepared using 100 grams of dried powder in 500 ml of purified water after refluxing for 5 hours. The obtained liquid was cleaned several times to eliminate contaminations.

Gamry electrochemical workstation was used to carry out the electrochemical experiments. A traditional three electrode was used together in a cell consisting of a reference electrode, counter electrode and working electrode, respectively. Prior to the start of each experiment, the set up with the complete cell and corrosive solution was permitted to be steady for 30 minutes. This was conducted to get a stable potential to ensure smooth running of experiments [13]. Electrochemical Impedance Spectroscopy (EIS) experiments were conducted in the  $0.0001 \text{ Hz}$  to  $10 \text{ MHz}$  frequency range. The chosen amplitude was  $10 \text{ mV}$  and the temperature was retained at  $308 \pm 1 \text{ K}$  with the help of a water bath. Echem analyst software that comes with Gamry instrument was used to analyze the obtained results from the tests conducted.

The potentiodynamic polarization tests were performed at  $-250 \text{ mV}$  to  $+250 \text{ mV}$  with a scan rate of  $1 \text{ mV s}^{-1}$  [14]. The chosen scan rate is neither too slow nor too fast and it gives the smooth curve without much disturbances. The curves of the anodic and cathodic slopes were selected to detect the corrosion current density ( $i_{\text{corr}}$ ), corrosion potential ( $E_{\text{corr}}$ ) and other parameters. For each test, a new metal sample was used and the solution was kept unstirred. All the tests were repeated to ensure the reproducible results.

To test the hydrophilic and hydrophobic behavior of the steel surface, contact angle experiments were done using the drop technique. All the tests were performed using DSA100 Kruss instrument and prior to each test the electrodes were cleaned cautiously to prevent contaminations. The scanning electron microscopy (SEM) was done to detect the changes at the external area of the metal. SEM was

conducted using Tescan machine. The samples were washed with sodium bicarbonate solution to remove the corrosion products followed by distilled water prior to surface exposure.

### 3. RESULTS AND DISCUSSION

#### 3.1. Weight loss experiments

##### 3.1.1 Influence of AS concentration

The values of the inhibition efficiency ( $\eta\%$ ) achieved through weight loss experiments for diverse concentrations of AS in 1 M H<sub>2</sub>SO<sub>4</sub> are given in Table 1. The corrosion tests were executed on triplicate samples and their mean rate of corrosion was determined. The following equation was followed to determine the rate of corrosion ( $C_R$ ) [15]:

$$C_R \text{ (mm/y)} = \frac{8.76W}{atD} \quad (1)$$

where  $W$  be the weight loss,  $a$  be the total area,  $t$  be the time of immersion (3 hours) and  $D$  be density of mild steel in (gcm<sup>-3</sup>). The subsequent equation was used to determine the inhibition efficiencies ( $\eta\%$ ):

$$\eta\% = \frac{WL_b - WL_i}{WL_b} \times 100 \quad (2)$$

$WL_i$  and  $WL_b$  are the corrosion rates with and without AS, respectively.

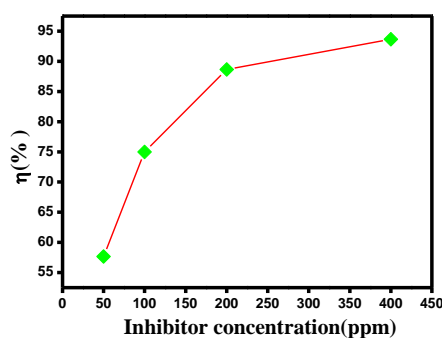


**Figure 2.** Effect of change in the inhibitor concentration versus Inhibition efficiency ( $\eta\%$ ) at 30 °C.

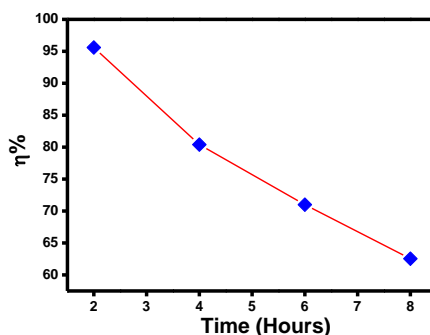
The efficiency ( $\eta\%$ ) tend to rise with increase in the AS concentration and corrosion rate tend to decrease with rise in inhibitor concentration as exposed in Fig. 2 and Table 1. As inhibition efficiency can be correlated to the surface coverage, with escalation in efficiency surface coverage also increases. Maximum inhibition efficiency is found to be 94% for 400 ppm AS. The efficiency did not exceed much after the concentration was increased to 500 and 600 ppm, so 400 is chosen as the optimum concentration for the AS. The adsorption of AS on the steel surface took place through the heteroatoms present in the solution that formed a coating on the steel surface and blocked the corrosive media [16, 17].

**Table 1.** Corrosion data for mild steel in 1 M H<sub>2</sub>SO<sub>4</sub> in the absence and presence of AS.

AS concentration (ppm)	Weight loss (mg cm <sup>-2</sup> )	C <sub>R</sub> (mm y <sup>-1</sup> )	$\eta$ (%)	Surf. Coverage ( $\theta$ )
1 M H <sub>2</sub> SO <sub>4</sub>	29.0	107.5	-	-
50	12.6	35.6	57	0.57
100	07.3	23.3	75	0.75
200	03.2	11.8	89	0.89
400	01.6	05.8	94	0.94

### 3.1.2. Influence of Immersion time

The influence of immersion time on the efficiency of AS to inhibit mild steel corrosion in 1 M H<sub>2</sub>SO<sub>4</sub> is revealed in Fig. 3. It is observed that the inhibition efficiency declines with growing time period from 2 to 8 hours. The phenomenon points that desorption of the AS particles from metal surface occurs with rise in the time period. The corrosive solution of sulphuric acid is able to penetrate the inhibitor film and attack the steel surface.

**Figure 3.** Effect of immersion time on corrosion of mild steel in 1 M H<sub>2</sub>SO<sub>4</sub> with 400 ppm AS at 30°C.

### 3.1.3. Acid concentration influence

The different concentration of sulphuric acid was prepared from 0.5 to 2.0 M to analyze the change in the efficiency of AS inhibitor as is exposed in Fig. 4. The inference is strong that with the modification in the concentration of acid from 0.5 M to 2.0 M, inhibition efficiency varied from 96.3% to 72.1%. The alteration in the efficiency with rising concentration of acid points toward the weak bonding of the AS particles with steel surface or less effective nature that could be ruptured due to the presence of acidic media. It could also be deterred as with rise in acid concentration the concentration of the inhibitor used should also be increased for better inhibition efficiency.

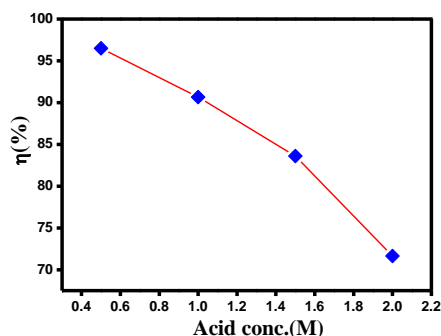


**Figure 4.** Effect of acid concentration versus inhibition efficiency on corrosion of mild steel at 30°C.

### 3.1.4. Influence of Temperature

The influence of temperature on the corrosion of mild steel in 1 M H<sub>2</sub>SO<sub>4</sub> solution with and without 400 ppm AS was conducted using weight loss technique for a duration of 3 hours. The temperature was varied from 308 to 338 K.

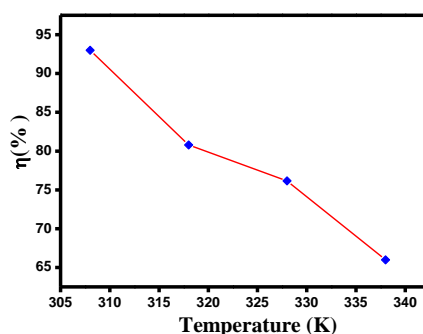


**Figure 5.** Effect of different temperature versus inhibition efficiency on corrosion of mild steel in 1 M H<sub>2</sub>SO<sub>4</sub>.

Fig. 5 shows the temperature versus inhibition efficiency and corrosion rate diagram. One can keenly observe from the figure that with an rise in temperature the inhibition efficiency decreases and likewise the corrosion rate increases at optimum concentration (400 ppm) of AS. This decrease in inhibition efficiency at high temperature suggests that the AS cannot perform at high temperature conditions. The increase in corrosion rate also points towards the aggressiveness of acidic solution at high temperatures. This may be due to desorption of the AS particles from the mild steel surface that let the corrosive solution to attack the steel surface thereby increasing the rate of corrosion [18]. Also, it may be attributed to the thin film of the AS that was removed or blistered at high temperature.

### 3.2 Adsorption isotherm

The Arrhenius equation given below was followed to determine the activation energy of the system [19]:

$$C_R = \lambda \exp\left(\frac{-E_a}{RT}\right) \tag{3}$$

where  $C_R$  represents the rate of corrosion,  $\lambda$  be the constant,  $E_a$  represents the activation energy,  $R$  be the gas constant, and  $T$  be the temperature. The values of  $\log C_R$  (mpy) and  $1/T \times 10^{-3}$  (kelvin) were accounted for determination of activation energy as exposed in Fig. 6a. The transition state equation used is an alternative form of the Arrhenius equation [20]:

$$Rate = \frac{RT}{Nh} \exp\left(\frac{\Delta S^\circ}{R}\right) \exp\left(-\frac{\Delta H^\circ}{RT}\right) \tag{4}$$

where  $h$  represents Plank's constant,  $N$  be the Avogadro's number,  $\Delta S^\circ$  represents entropy and  $\Delta H^\circ$  represents enthalpy. A linear fit straight line is obtained from  $\log(C_R/T)$  versus  $1/T$  graph as exposed in Fig. 6b. The values of  $\Delta S^\circ$  and  $\Delta H^\circ$  were determined from the slope and intercept as tabulated in table 2.

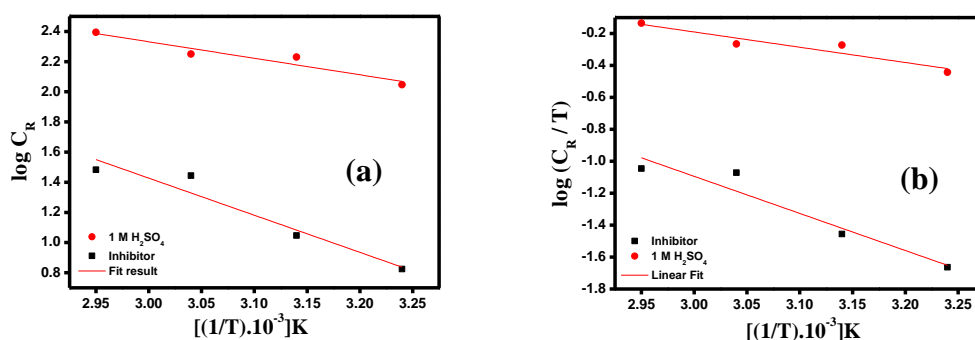


**Figure 6.** Arrhenius plots of (a)  $\log C_R$  versus  $1/T$  and (b)  $\log C_R/T$  versus  $1/T$  for mild steel in acidic media.

The data in Table 2 displays that activation energy ( $E_a$ ) of mild steel in 1 M  $\text{H}_2\text{SO}_4$  solution is greater in the presence of the AS. On the other hand, it is lower in the acidic media without AS signifying that the inhibitor drops the inhibition efficiency at elevated temperature [21-24]. The value of activation energy ( $E_a$ ),  $21.0 \text{ kJ mol}^{-1}$  for 1 M  $\text{H}_2\text{SO}_4$  and  $62.7 \text{ kJ mg}^{-1}$  of 400 ppm inhibitor was determined from the slope of the straight line. The greater value of  $E_a$  in presence of AS is due to the very strong adsorption of AS particles on the steel surface. The molecules formed a strong film/complex with the metal surface that reduced the dynamic centers and served as a protective layer [25]. The values obtained for free energy of adsorption ( $\Delta G^\circ_{ads}$ ) shows a negative sign signifying the spontaneous nature of the corrosion process [26, 27]. The equation below was used to determine the values [28].

$$\Delta G^\circ_{ads} = -RT \ln K_{ads} \tag{5}$$

**Table 2.** The thermodynamic parameters  $E_a$ ,  $\Delta H^\circ$  and  $\Delta S^\circ$  for mild steel in 1 M  $H_2SO_4$  with and without AS.

AS concentration (ppm)	$E_a$ (kJ mol <sup>-1</sup> )	$-\Delta H^\circ$ (kJ mol <sup>-1</sup> )	$-\Delta S^\circ$ (J mol <sup>-1</sup> K <sup>-1</sup> )	$K_{ads}$ (M <sup>-1</sup> )	$-\Delta G^\circ_{ads}$ (kJ mol <sup>-1</sup> )
1 M $H_2SO_4$	21.0	19.3	134.2	08,092	-
50	29.4	25.6	97.4	11,801	32.4
100	46.9	43.3	72.2	14,478	34.1
200	53.2	55.9	53.7	18,663	34.6
400	62.7	67.1	27.2	24,580	35.7

$$K_{ads} = \frac{\theta}{C(1-\theta)} \quad (6)$$

where,  $\theta$  be the degree of coverage,  $C$  represents concentration of AS in ppm,  $R$  be the constant and  $T$  represents temperature. The  $\Delta G^\circ_{ads}$  value of the AS is found to be 35.7 kJ/mol. This value is lesser than -40 kJ/mol demonstrating that AS is adsorbed physically on the surface of mild steel [29]. The negative parameter of  $\Delta G^\circ_{ads}$  specified the impulsive adsorption of AS particles on the steel surface [30]. Higher values of  $K_{ads}$  represents better adsorption of the AS particles on the steel surface as it is related to the free energy.

Chemical compounds establish corrosion mitigation by adsorption. The adsorption of AS is inclined by the natural structures of molecules present in the root extract, nature and external charge of metal, and type of aggressive media [31]. The physical adsorption requires the presence of electrically charged metal surface and charged particles in the bulk of solution. The steel surface consists of unoccupied d orbitals and lower energy orbital, through which it can form complex with the heteroatoms present in the AS molecule [32].

The statistics for the interaction between the AS particles and steel surface can be reflected by the isotherm of adsorption. The process is based on a chemical reaction where the AS molecule displaces the water molecule present on the steel surface and get adsorbed [33].



where,  $\text{Org}_{(sol)}$  and  $\text{Org}_{(ads)}$  are the AS particles in the solution and adsorbed particles on the steel surface,  $\text{H}_2\text{O}_{(ads)}$  represents the water molecules,  $x$  be the size ratio. The surface coverage values obtained through weight loss, EIS and polarization experiments were accounted to fit several isotherms of adsorption such as Flory Huggins, Langmuir, Temkin, and Frumkin. The good fit of these isotherms can signify the nature of adsorption by the AS molecules. Surface coverage ( $\theta$ ) can be correlated to the concentration of AS inhibitor as shown below:

$$\theta = \frac{bC_{inh}}{1+bC_{inh}} \quad (\text{Langmuir isotherm}) \quad (8)$$

$$\exp(-2a\theta) = KC_{inh} \quad (\text{Temkin isotherm}) \quad (9)$$

where,  $b$  defines the adsorption,  $a$  represents molecular interaction,  $K$  be the equilibrium constant. Among all the isotherm of adsorption, Langmuir showed the best and linear fit to the surface coverage

parameters as depicted in Fig. 7. The values of regression coefficient was close to 1 for all the experimental data that signifies the good adsorption of AS particles on the steel in acidic media.

All the acquired fits are in good agreement with each other. This justifies the adsorption of AS molecules on the mild steel surface that prevents its corrosion from 1 M H<sub>2</sub>SO<sub>4</sub> solution.

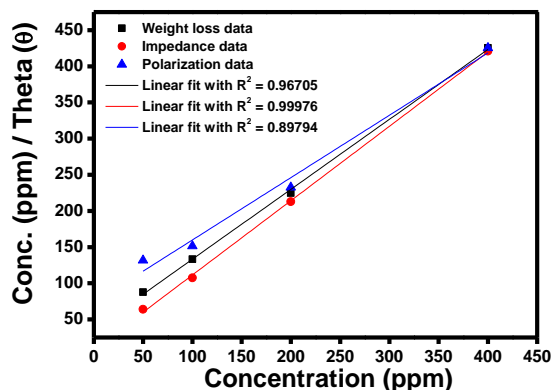


Figure 7. Linear fit results of Langmuir isotherm for adsorption of AS on mild steel in 1 M H<sub>2</sub>SO<sub>4</sub>.

### 3.2 Electrochemical measurements

#### 3.2.1. Electrochemical impedance spectroscopy (EIS) tests

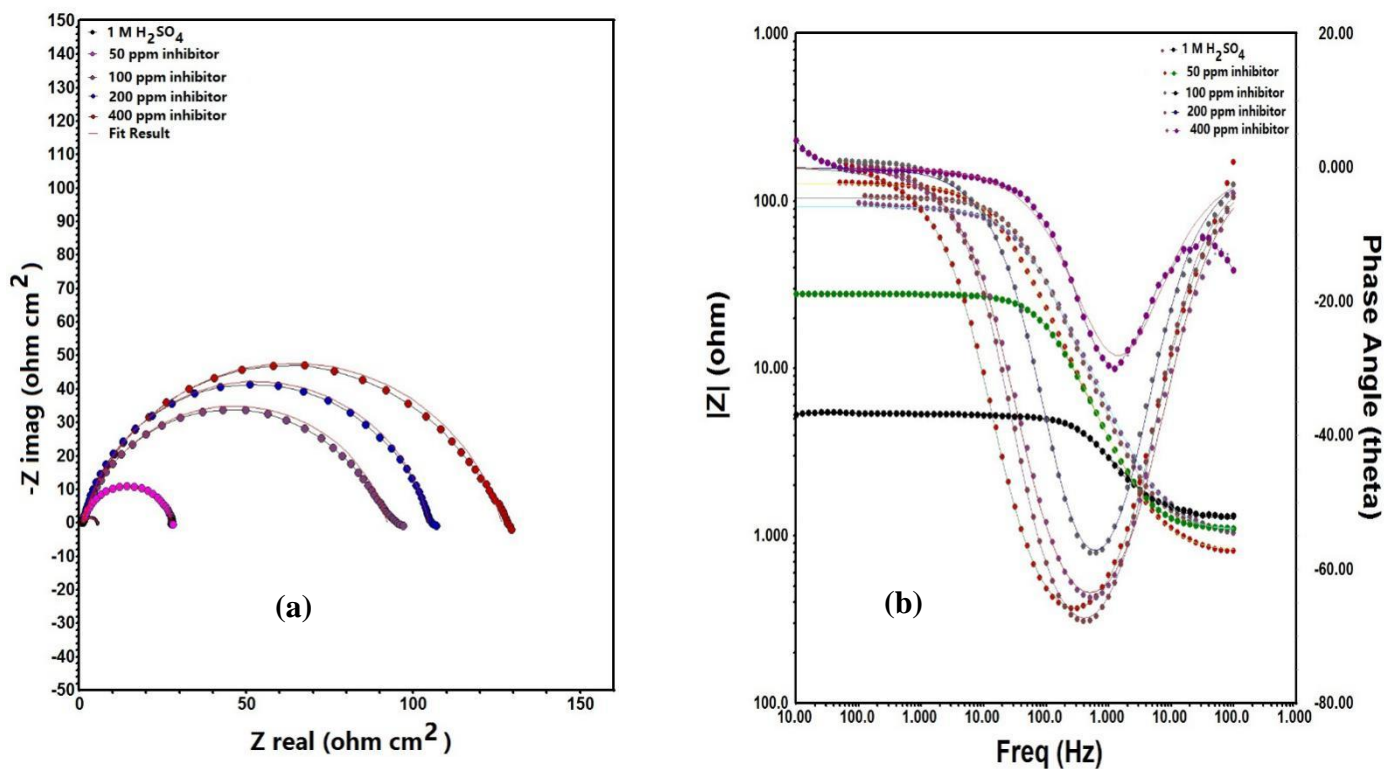
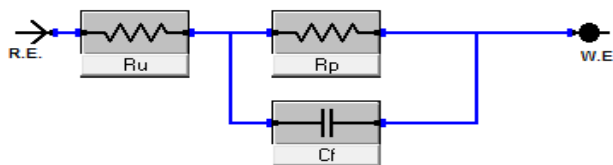


Figure 8. (a) Nyquist and (b) bode-phase angle plots for mild steel in 1 M H<sub>2</sub>SO<sub>4</sub> with and without AS at 30°C.



**Figure 9.** Corresponding Randle's circuit used to fit Nyquist plots in 1 M H<sub>2</sub>SO<sub>4</sub> with different concentrations of AS.

Nyquist figures of mild steel in 1 M H<sub>2</sub>SO<sub>4</sub> with and without AS are specified in Fig. 8a, and it can be detected that the width of the semicircle rises with increasing AS adsorption. This rise in semicircles of capacitance recommends that the mitigation behavior of AS is due to its adsorption on the mild steel surface deprived of varying the corrosion process [34-38]. Furthermore, Fig. 8a shows the higher and lower frequency regions with similar capacitance but with different diameter.

**Table 3.** Electrochemical impedance parameters for mild steel in 1 M H<sub>2</sub>SO<sub>4</sub> solution with and without AS

AS concentration (ppm)	$R_{ct}$ ( $\Omega \text{ cm}^2$ )	$n$	$Y_0$ ( $10^{-6} \Omega^{-1} \text{ cm}^{-2}$ )	$C_{dl}$ ( $\mu\text{F cm}^{-2}$ )	$\eta\%$	Slope	Phase angle
Blank	07.2	0.567	266.2	97.5	-	0.432	34.9
50	32.9	0.589	238.5	75.3	78	0.476	58.3
100	103.4	0.627	197.1	57.2	93	0.504	62.9
200	119.7	0.688	142.8	35.7	94	0.615	64.6
400	141.5	0.726	99.6	27.5	95	0.649	66.7

In the bode plots (Fig. 8b), the slope values tend to increase in existence of AS than in its nonexistence (Table 3). This indicates the inhibition action of AS on mild steel surface. In phase angle plots (Fig. 8b), at the intermediate frequency the height of the peak and phase angle values increases as the AS concentration increases. The highest peak at 66.7° (400 ppm) AS concentration for mild steel was observed and reported in Table 3. This is an indication of the development of protective obstacle that causes the isolation of the steel surface from the aggressive solution [39, 40]. Thus, in other words adsorption of the AS particles over the steel plays the significant part, which ultimately increased its corrosion resistance property.

The results of the impedance parameters achieved after fitting the curves of Nyquist with the corresponding circuit (Fig. 9) are tabulated in Table 3. The Randle's equivalent circuit model contains capacitance CPE, which is in parallel with charge transfer resistance ( $R_{ct}$ ) and they are overall in series

with the solution resistance ( $R_s$ ). The frequency dependent distribution of the current density along the metal surface can be compensated by using the CPE in place of pure capacitor [41, 42]. The CPE impedance ( $Z_{CPE}$ ) was calculated using the below equation:

$$Z_{CPE} = Y_0 [j\omega^\alpha]^{-1} \quad (10)$$

where  $j$  be an imaginary number ( $j = \sqrt{-1}$ ),  $Y_0$  be the admittance and constant for CPE,  $\omega$  be the angular frequency, and  $\alpha$  be the phase change [43]. The addition of AS molecules causes the modification of the capacitance parameters owing to the adsorption at the steel-liquid interface. Thus, it become important to calculate the double layer capacitance ( $C_{dl}$ ) data, because the representation of  $C_{dl}$  by CPE and  $Y_0$  is not accurate when the values of  $\alpha$  is less than 1. The accurate relationship between the  $C_{dl}$  and CPE can be calculated using the equation [44]:

$$C_{dl} = Y_0^{1/\alpha} \left[ \frac{1}{R_s} + \frac{1}{R_{ct}} \right]^{(\alpha-1)/\alpha} \quad (11)$$

For electrochemical impedance the effectiveness of AS was evaluated using the equation below:

$$\eta\% = \frac{R_{ct(i)} - R_{ct(b)}}{R_{ct(i)}} \times 100 \quad (12)$$

where  $R_{ct(i)}$  and  $R_{ct(b)}$  represent the values of charge transfer resistance with and without AS in 1 M  $H_2SO_4$  correspondingly [45]. According to the Table 3, the  $R_{ct}$  values rises and  $C_{dl}$  declines with the addition of the AS to the corrosive solution. This can be ascribed to the adsorption of AS fragments over the mild steel surface and reduces the direct connection between the metal and hostile solution [46]. In addition to this, the increasing values of the efficiency of inhibition in existence of AS further support the protection ability of AS.

### 3.2.2. Polarization tests

Fig. 10 depicts the potentiodynamic polarization pictures of the mild steel with and without AS in 1 M  $H_2SO_4$  media. As can be seen from the figure that both the hydrogen evolution (cathodic) and steel dissolution (anodic) processes were affected after the accumulation of AS in the acidic solution [47]. Although, the overall mechanism was not affected by the addition of the AS as neither the anodic nor the cathodic shift was observed. The polarization data such as  $E_{corr}$ ,  $i_{corr}$ , and anodic ( $\beta_a$ ), and cathodic ( $-\beta_c$ ) slopes were determined from the experiments done using the equation below [48]:

$$\eta_p\% = \frac{i_{corr} - i_{corr(i)}}{i_{corr}} \times 100 \quad (13)$$

$i_{corr}$  and  $i_{corr(i)}$  signify the corrosion current density with and without AS. The little shift towards cathodic region after the addition of AS, may be owing to the fact that the adsorption of AS molecules on the steel surface hindered the corrosive media attack on the working electrode as is evident from the  $-\beta_c$  values reported in Table 4 [49]. So, the addition of AS in the acidic solution did not changed the overall corrosion mechanism. There was also a little change in the anodic values of  $\beta_a$  that may be endorsed to the development of protective layer of AS molecules on the mild steel surface that further blocked the active centers present on the surface, thereby slowing the dissolution process [50, 51].

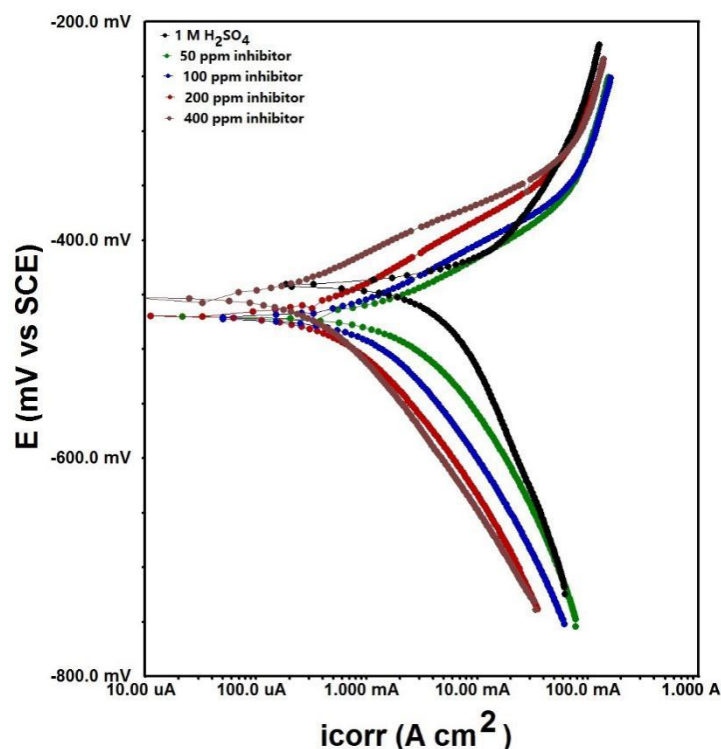


**Figure 10.** Polarization curves for mild steel in 1 M H<sub>2</sub>SO<sub>4</sub> in presence of different concentrations of AS at 30°C.

**Table 4.** Electrochemical polarization parameters for mild steel in 1 M H<sub>2</sub>SO<sub>4</sub> solution with and without AS.

AS (ppm)	$E_{\text{corr}}$ (mV/SCE)	$I_{\text{corr}}$ (mA cm <sup>-2</sup> )	$\beta_a$ (mV dec <sup>-1</sup> )	$\beta_c$ (mV dec <sup>-1</sup> )	$\eta_p$ (%)
1 M H <sub>2</sub> SO <sub>4</sub>	-421	285	130	128	–
50	-426	177	108	92	38
100	-431	96	93	78	66
200	-433	41	77	56	86
400	-425	18	127	121	94

The maximum inhibition efficiency of 94% at 400 ppm concentration was observed suggesting the lower corrosion rate in presence of AS. The corrosion potential did not showed much variation or shift and was quite stable. The conclusions of research papers suggests that if the shift or movement in corrosion potential is  $\geq 85$  mV with reference to the blank (1M H<sub>2</sub>SO<sub>4</sub>) solution, then only an AS can be classified into anodic or cathodic inhibitor [52, 53]. But, from Fig. 10 and Table 4, the shift is very evident and is found to be 12 mV. So, based on this theory AS can be classified as mixed type AS.

### 3.3 Surface Characterization

#### 3.3.1. Contact Angle

To detect the surface behavior of mild steel with and without AS, contact angle tests were conducted. Contact angle tests can provide essential information regarding the hydrophilic and

hydrophobic nature of the steel. The samples were degreased and cleaned several times before test to remove all kinds of contaminants. A baseline establishment was completed after several attempts to perform the tests smoothly using the sessile drop technique. The solution was dropped using a syringe and was repeated for three times to make sure the reproducibility of the tests. The 1 M  $\text{H}_2\text{SO}_4$  solution without AS recorded a lower contact angle of  $11.6^\circ$  as shown in Fig. 11. This may be endorsed to the surface of the steel that is in direct connection with the corrosive environment. The corrosive solution can directly attack the steel surface and due to this water loving nature it is termed as hydrophillic surface. Whereas, when the AS was added in the solution, it formed a film at the steel surface and due to the presence of this film the contact angle begin to increase. It was  $102.4^\circ$  at 400 ppm concentration suggesting that the film blocked the corrosive solution to reach at the steel surface and this nature is termed as hydrophobic behavior of the surface. So, the surface was hydrophillic without AS and hydrophobic with AS. This justifies the good inhibiting action of AS in 1 M  $\text{H}_2\text{SO}_4$ .

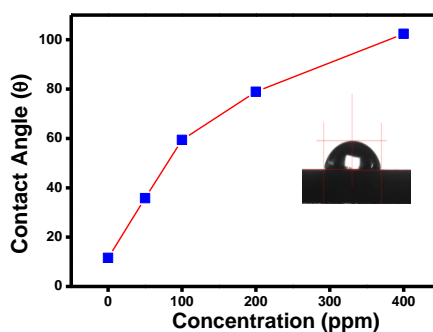


**Figure 11.** Contact angle for mild steel 1 M  $\text{H}_2\text{SO}_4$  in presence and absence of AS at  $30^\circ\text{C}$ .

### 3.3.2 SEM characterization

To observe the range of protection of the steel surface by AS, the morphology of mild steel surface submerged in 1 M  $\text{H}_2\text{SO}_4$  without and with 400 ppm AS was checked using SEM. In order to get a clear picture of AS action the steel surface without AS was exposed to SEM first and the result is represented in Fig. 12a. The surface is very rough, corroded and irregular. The corrosive solution attacked the mild steel surface and due to oxidation the steel formed rust after corroding. While, in presence of AS the steel surface was smooth, regular and less corroded as shown in Fig. 12b. The abraded lines can be seen and the surface is much better than without AS. This proposes that the AS formed a shielding layer on the steel surface that inhibited the corrosion progression by blocking the corrosive solution from attacking the metal surface.

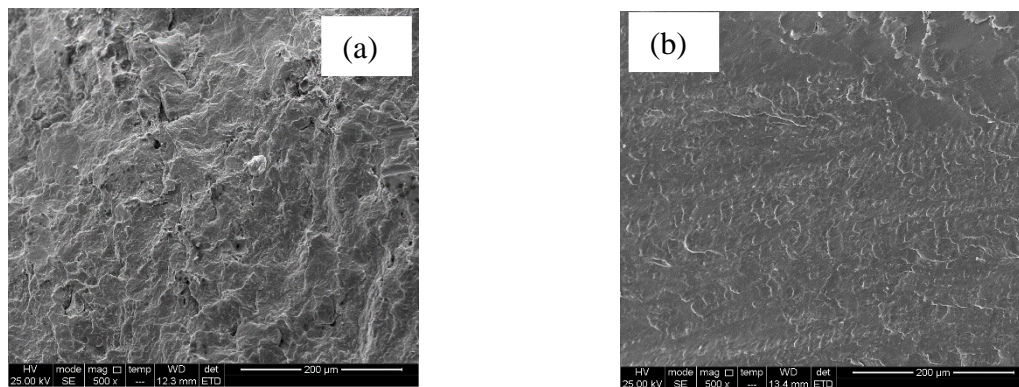


**Figure 12.** SEM images for mild steel (a) 1 M H<sub>2</sub>SO<sub>4</sub>, and (b) 400 ppm AS at 30°C.

#### 4. CONCLUSIONS

- Stem extract of *Angelica sinensis* can be used as potential corrosion AS for mild steel in 1 M H<sub>2</sub>SO<sub>4</sub> solution.
- The weight loss tests showed that the corrosion rate declines with AS while the inhibition efficiency rises.
- The impedance studies revealed that the charge transfer resistance increases in presence of AS and double layer capacitance values decreases.
- Polarization studies pointed that the anodic and cathodic shifts are mixed type in nature, so the AS could be categorized in mixed class AS.
- Contact angle showed the hydrophobic nature of the steel in presence of AS. SEM showed the smooth mild steel surface with less roughness in presence of AS.

#### ACKNOWLEDGMENT

Authors are thankful to the Sichuan 1000 Talent Fund, financial assistance provided by the Youth Scientific and Innovation Research Team for Advanced Surface Functional Materials, Southwest Petroleum University number-2018CXTD06 and open fund project number-X151517KCL42.

#### References

1. M. Finšgar, J. Jackson, *Corros. Sci.*, 86 (2014) 17.
2. R. Wang, S. Luo, *Corros. Sci.*, 68 (2013) 119.
3. M.A. Bedair, M.M.B. El-Sabbah, A.S. Fouda, M. Elaryian, *Corros. Sci.*, 128 (2017) 45.
4. K.C. Emregul, A. Abbas Aksut, *Corros. Sci.*, 42 (2008) 2051.
5. M.M. Solomon, S.A. Umoren, I.I. Udoso, A.P. Udoh, *Corros. Sci.*, 52 (2010) 1317.
6. L. Zhou, Y.L. Lv, Y.X. Hu, J.H. Zhao, X. Xia, X. Li, *J. Mol. Liq.*, 249 (2018) 179.
7. A. A. Olajire, *J. Mol. Liq.*, 248 (2017) 775.
8. Ambrish Singh, K. R. Ansari, M. A. Quraishi, Hassane Lgaz and Yuanhua Lin, *J. Alloys Comp.*, 762 (2018) 347.
9. A. Singh, I. Ahamad, M. A. Quraishi, *Arab. J. Chem.*, 9 (2016) S1584.

10. A. Yousefi, S. Javadian, N. Dalir, J. Kakemam, J. Akbari, *RSC Adv.*, 5 (2015) 11697.
11. K. Azzaoui, E. Mejdoubi, S. Jodeh, A. Lamhamdi, E. Rodriguez-Castellón, M. Algarra, A. Zarrouk, A. Errich, R. Salghi, H. Lgaz, *Corros. Sci.*, 129 (2017) 70.
12. Liu Dongling, Wang Yinquan, Tian Ling, *Intech publications*, DOI: 10.5772/66739 (2017).
13. A.A. Khadom, A.N. Abd, N.A. Ahmed, *South Afri. J. Chem. Eng.*, 25 (2018) 13.
14. E.B. Ituen, O. Akaranta, S.A. Umoren, *J. Mol. Liq.*, 246 (2017) 112.
15. M.M. Askari, S.G. Aliofkhazraei, A. Hajizadeh, *J. Nat. Gas Sci. Eng.*, 58 (2018) 92.
16. A. Singh, Y. Lin, W. Liu, D. Kuanhai, J. Pan, B. Huang, C. Ren, D. Zeng, *J. Tai. Inst. Chem. E.*, 45 (2014) 1918.
17. A. Singh, Y. Lin, M. A. Quraishi, O. L. Olasunkanmi, O. E. Fayemi, Y. Sasikumar, B. Ramaganthan, I. Bahadur, I. B. Obot, A. S. Adekunle, M. M. Kabanda, E. E. Ebenso, *Molecules*, 20 (2015) 15122.
18. Ambrish Singh, Y. Lin, W. Liu, S. Yu, J. Pan, C. Ren, D. Kuanhai, *J. Ind. Eng. Chem.*, 20 (2014) 4276.
19. D.D. Macdonald, S. Real, M. Urquidi-Macdonald, *J. Electrochem. Soc.*, 135 (1988) 2397.
20. D. Chu, R.F. Savinel, *Electrochim. Acta*, 36 (1991) 1631.
21. A.M. Abdel-Gaber, E. Khamis, H. Abo-ElDahab, Sh. Adeel, *Mater. Chem. Phys.*, 109 (2008) 297.
22. S.S. Zhang, T.R. Jow, *J. Power Source*, 109 (2002) 458.
23. A.A. El Hosary, R.M. Saleh, A.M. Shams El Din, *Corros. Sci.*, 12 (1972) 897.
24. M.A. Quraishi, A. Singh, V.K. Singh, D.K. Yadav, A.K. Singh, *Mater. Chem. Phys.*, 122 (2010) 114.
25. A. Singh, I. Ahamad, V.K. Singh, M.A. Quraishi, *J. Sol. State Electrochem.*, 15 (2011) 1087.
26. G. Gunasekaran, L.R. Chauhan, *Electrochim. Acta*, 49 (2004) 4387.
27. Ambrish Singh, K.R. Ansari, Jiyaul Haque, Parul Dohare, Hassane Lgaz, Rachid Salghi, M.A. Quraishi, *J. Taiwan Inst. Chem. E.*, 82 (2018) 233.
28. A.Y. El-Etre, M. Abdallah, Z.E. El-Tantawy, *Corros. Sci.*, 47 (2005) 385.
29. Ambrish Singh, Y. Lin, I. B. Obot, E. E. Ebenso, K. R. Ansari, M. A. Quraishi, *Appl. Surf. Sci.*, 356 (2015) 341.
30. E.E. Oguzie, *Corros. Sci.*, 49 (2007) 1527.
31. A. Singh, Y. Lin, E. E. Ebenso, W. Liu, B. Huang, *Int. J. Electrochem. Sci.*, 9 (2014) 5993.
32. A. Singh, E. E. Ebenso, M. A. Quraishi, Y. Lin, *Int. J. Electrochem. Sci.*, 9 (2014) 7495.
33. A. Singh, I. Ahamad, V. K. Singh, M. A. Quraishi, *Chem. Engg. Comm.*, 199 (2012) 63.
34. Z. Tao, S. Zhang, W. Li, B. Hou, *Ind. Eng. Chem. Res.*, 50 (2011) 6082.
35. E.S. Ferreira, C. Giacomelli, F.C. Giacomelli, A. Spinelli, *Mater. Chem. Phys.*, 83 (2004) 129.
36. D.D. Macdonald, *Electrochim. Acta*, 35 (1990) 1509.
37. K.K. Lee, K.B. Kim, *Corros. Sci.* 43 (2001) 561.
38. A. Singh, K.R. Ansari, A. Kumar, W. Liu, C. Songsong, Y. Lin, *J. Alloys Comp.*, 712 (2017)121.
39. A. Singh, Y. Lin, E. E. Ebenso, W. Liu, J. Pan, B. Huang, *J. Ind. Eng. Chem.*, 24 (2015) 219.
40. E. Khamis, *Corrosion*, 46 (1990) 476.
41. A. Singh, Yuanhua Lin, K. R. Ansari, M. A. Quraishi, E. E. Ebenso, Songsong Chen, W. Liu, *Appl. Surf. Sci.*, 359 (2015) 331.
42. A. Singh, Y. Caihong, Y. Yaocheng, N. Soni, Y. Wu, Y. Lin, *ACS Omega*, 4 (2019) 3420.
43. A. Singh, N. Soni, Y. Deyuan, A. Kumar, *Res. Phys.*, 13 (2019) 102116.
44. X. Xu, A. Singh, Z. Sun, K. R. Ansari, Y. Lin, *R. Soc. Open Sci.*, 4 (2017) 170933.
45. P. Singh, A. Singh, M.A. Quraishi, *J. Taiwan Inst. Chem. E.*, 60 (2016) 588.
46. Y. Lin, A. Singh, E. E. Ebenso, Y. Wu, C. Zhu, H. Zhu, *J. Taiwan Inst. Chem. E.*, 46 (2015) 214.
47. A. Singh, M. Talha, X. Xu, Z. Sun, Y. Lin, *ACS Omega*, 2 (2017) 8177.
48. A. Singh, Y. Lin, I. B. Obot, E. E. Ebenso, *J. Mol. Liq.*, 219 (2016) 865.
49. A. Singh, K. R. Ansari, X. Xu, Z. Sun, A. Kumar, Y. Lin, *Sci. Report.*, 7 (2017) 14904.
50. P. E. Alvarez, M. V. Fiori-Bimbi, A. Neske, S. A. Brandán, C. A. Gervasi, *J. Ind. Eng. Chem.*, 58

(2018) 92.

51. H. Feng, A. Singh, Y. Wu, Y. Lin, *New J. Chem.*, 42 (2018) 11404.

52. N. Li, S. Tang, Y. Rao, J. Qi, Q. Zhang, D. Yuan. *Electrochim. Acta*, 298 (2019) 59.

53. X. Wang, Z. Peng, S. Zhong, *Int. J. Electrochem. Sci.*, 13 (2018) 8970.

© 2019 The Authors. Published by ESG ([www.electrochemsci.org](http://www.electrochemsci.org)). This article is an open access article distributed under the terms and conditions of the Creative Commons Attribution license (<http://creativecommons.org/licenses/by/4.0/>).